Available online at www.sciencedirect.com

SciVerse ScienceDirect

Ceramics International 38 (2012) 6015–6020

CERAMICS INTERNATIONAL

www.elsevier.com/locate/ceramint

Short communication

Dielectric properties of Si_3N_4–SiCN composite ceramics in X-band

Quan Li, Xiaowei Yin *, Liyun Feng

Science and Technology on Thermostructural Composite Materials Laboratory, Northwestern Polytechnical University, Xi'an 710072, China

Received 16 January 2012; received in revised form 23 February 2012; accepted 19 March 2012
Available online 28 March 2012

Abstract

Si_3N_4–SiCN composite ceramics were successfully fabricated through precursor infiltration pyrolysis (PIP) method using polysilazane as precursor and porous Si_3N_4 as preform. After annealed at temperatures varying from 900 °C to 1400 °C, the phase composition of SiCN ceramics, electrical conductivity and dielectric properties of Si_3N_4–SiCN composite ceramics over the frequency range of 8.2–12.4 GHz (X-band) were investigated. With the increase of annealing temperature, the content of amorphous SiCN decreases and that of N-doped SiC nano-crystals increases, which leads to the increase of electrical conductivity. After annealed at 1400 °C, the average real and imaginary permittivities of Si_3N_4–SiCN composite ceramics are increased from 3.7 and 4.68×10^{-3} to 8.9 and 1.8, respectively. The permittivities of Si_3N_4–SiCN composite ceramics show a typical ternary polarization relaxation, which are ascribed to the electric dipole and grain boundary relaxation of N-doped SiC nano-crystals, and dielectric polarization relaxation of the in situ formed graphite. The Si_3N_4–SiCN composite ceramics exhibit a promising prospect as microwave absorbing materials.

Keywords: C: Dielectric property; D. Si_3N_4; D. SiC nano-crystal; Polymer derived ceramics

1. Introduction

In recent years, electromagnetic wave absorption materials have attracted considerable attentions because of their wide application in the electrical and electronic fields [1]. Magnetic powders such as nickel [2], ferrite and cobalt [3] can be used to fabricate microwave absorption materials. However, such magnetic microwave absorption materials cannot be used at temperatures exceeding their Curie points. For microwave absorption materials used at high temperatures, the microwave absorption mechanism is mainly dielectric loss.

Silicon carbide (SiC) ceramic is a wide band gap semiconductor which has many practical and potential applications in electromagnetic wave absorption at severe environments. The dielectric properties of various SiC materials including SiC powders [4], SiC nanofibers [5], SiC foams [6], and SiC matrix composites [7] have been investigated. However, the low electrical conductivity of pure SiC results in low dielectric loss. In order to improve its dielectric loss, the doped SiC nano-crystal materials have been studied, which exhibits much higher dielectric loss than pure SiC due to the formation of charged defects and a great deal of grain boundaries [8–11].

Polymer-derived SiCN (PDC-SiCN) ceramics can be turned into N-doped SiC-based ceramics [12]. The doping of SiC ceramics can be adjusted by controlling the annealing temperature, through which the dielectric properties can be designed. Besides, PDC-SiCN ceramics possess excellent thermal-stability, oxidation and creep resistances up to exceptionally high temperatures, etc. [13,14]. Considering the above advantages, the PDC-SiCN ceramics can be potentially used as electromagnetic wave absorption materials in severe environments. Up to now, few researches focus on the dielectric properties of PDC-SiCN ceramics.

In the present work, porous Si_3N_4 ceramic is used as preform, which is not only one kind of structural material for its excellent mechanical properties at elevated temperatures but also a functional material with low permittivity [15]. PDC-SiCN ceramics were introduced into the porous Si_3N_4 ceramic by precursor infiltration pyrolysis (PIP) at temperatures ranging from 900 °C to 1400 °C. The effects of annealing temperature on the electrical conductivity and dielectric properties of Si_3N_4–SiCN composite ceramics were investigated.

* Corresponding author. Tel.: +86 29 88494947; fax: +86 29 88494620.
E-mail addresses: yinxw@nwpu.edu.cn, liqvan841028@yahoo.cn (X. Yin).

0272-8842/$36.00
doi:10.1016/j.ceramint.2012.03.045

2. Experimental procedure

2.1. Materials preparation

A commercially available liquid-phased polysilazane was used as the precursor, and its chemical structure is shown in Fig. 1. First, the precursor was cross-liked at 250 °C for 2 h, and then pyrolyzed at 900 °C for 2 h. After pyrolysis, the as-received SiCN ceramics were annealed at 1200 °C and 1400 °C, respectively, in Ar atmosphere for 2 h in order to characterize the phase composition. Porous Si_3N_4 ceramic with porosity of 46% and density of 1.7 g/cm^3 was used as preform. The fabrication detail of porous Si_3N_4 ceramic was depicted elsewhere [16]. The as-received porous Si_3N_4 ceramic was machined into specimens and then ultrasonically cleaned in acetone and dried. The obtained Si_3N_4 specimens were dipped into polysilazane for 30 min each time. The temperatures at which the polymer in porous Si_3N_4 ceramics were cross-linked and annealed were the same as that of polymer alone. The obtained samples were designated as S1, S2, and S3, respectively, corresponding to the annealing temperatures of 900 °C, 1200 °C, and 1400 °C. As a comparison, a kind of SiC precursor, polycarbosilane [17], was cross-linked and then annealed at 1400 °C in Ar atmosphere for 2 h. The as received PDC-SiC was crushed into powder and then mixed with paraffin in order to characterize its dielectric properties. The ratio of powder in PDC-SiC/paraffin sample was 50 wt.% (20 vol.%).

2.2. Characterization

The phase compositions of the pure PDC-SiCN and SiC ceramic were analyzed by X-ray diffraction (XRD, Rigaku-D/max-2400, and Tokyo, Japan). The element composition of SiCN was analyzed by a combination of carbon–sulfur analyzer and oxygen–nitrogen analyzer (EMIA-320V/EMGA-620V, HORIBA Ltd., Hakata-ku, Japan).

The micrographs of Si_3N_4–SiCN composite ceramics were observed by scanning electron microscope (SEM, S-2700, and Hitachi, Japan). Density and open porosity of the Si_3N_4–SiCN composite ceramics were measured by Archimedes method according to ASTM C-20 standard. The complex permittivity of Si_3N_4–SiCN composite ceramics and that of SiC/paraffin sample with dimensions of 22.86 mm × 10.16 mm × 2.5 mm were measured in the frequency range of 8.2–12.4 GHz (X-band) using the vector network analyzer (VNA, MS4644A, Japan). The dielectric property of the porous Si_3N_4 ceramic with dimensions of ϕ50 mm × 4 mm was measured by resonant cavity method. The conductivity of Si_3N_4–SiCN composite ceramics was measured through I-V method (SCS 4200, Keithley, USA).

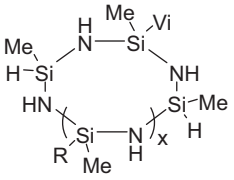

Fig. 1. Molecular structure of polysilazane, Me: Methyl; Vi: Vinyl.

3. Results and discussion

3.1. Phase and element composition of PDC-SiCN ceramics

In order to characterize the phase composition of SiCN, the XRD pattern of single PDC-SiCN powder was detected. Fig. 2(a) shows the XRD patterns of PDC-SiCN ceramics annealed at temperatures varying from 900 °C to 1400 °C. The SiCN ceramic is still amorphous when annealed at 1200 °C, and begins to crystallize at 1400 °C. The average grain size of β-SiC in SiCN ceramic is about 1.5 nm when annealed at 1400 °C. The grain size (D) is determined by using Scherrer equation:

$$D = \frac{k\lambda}{\beta \cos\theta} \quad (1)$$

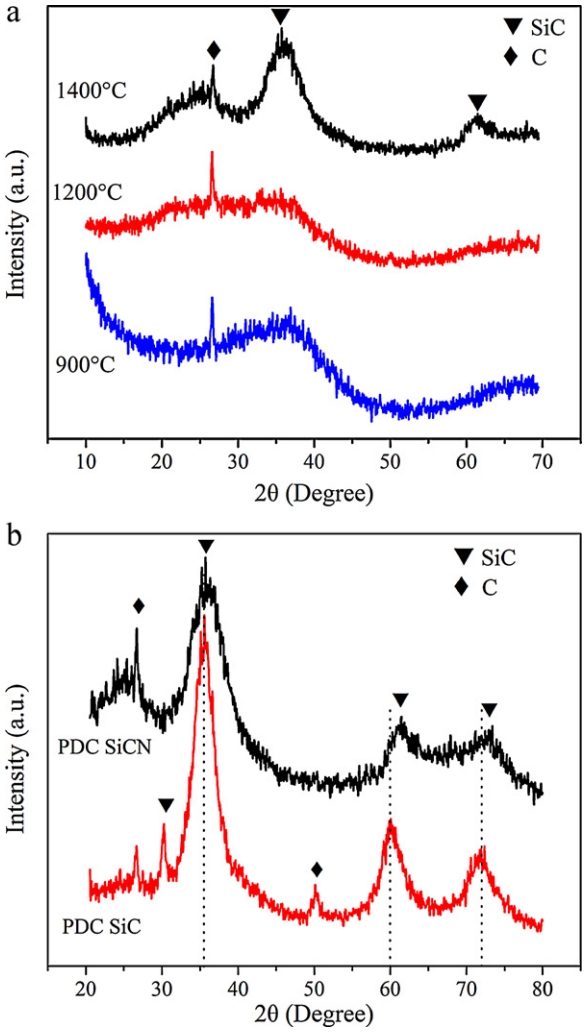

Fig. 2. XRD patterns of (a) polymer derived SiCN ceramic annealed at temperatures from 900 °C to 1400 °C respectively and (b) XRD patterns comparison of PDC-SiCN and SiC annealed at 1400 °C.

Table 1
The physical properties of porous Si_3N_4–SiCN ceramics annealed at different temperatures.

Sample	Temperature (°C)	Open porosity (%)	Bulk density (g/cm^3)	SiCN content (vol.%)	Conductivity (S/cm)	Empirical formula of PDC-SiCN ceramics
Porous Si_3N_4	–	46	1.7	0	$<10^{-13}$ [20]	–
S1	900	20	2.5	23	7.6×10^{-12}	$SiC_{1.18}N_{0.84}O_{0.06}$
S2	1200	21	2.5	23	4.9×10^{-10}	$SiC_{1.02}N_{0.81}O_{0.07}$
S3	1400	23	2.4	18	1.2×10^{-8}	$SiC_1N_{0.78}O_{0.05}$

where k is Scherrer constant (0.89), λ is wavelength of the incident ray, β is the angular line width at half maximum intensity in radians, and θ is Bragg's angle. No phase containing nitrogen element (N) can be detected in the XRD spectra of SiCN. As a comparison, the phase composition of PDC-SiC annealed at 1400 °C was characterized. Fig. 2(b) shows the difference of PDC-SiCN and PDC-SiC annealed at 1400 °C in XRD pattern. The peaks of β-SiC grains also appear in PDC-SiC. However, the peaks are much stronger in intensity and sharper in shape compared with that of β-SiC in PDC-SiCN. The average grain size of β-SiC grains in PDC-SiC is about 2.7 nm. Obviously, the XRD peaks of SiC in PDC-SiCN shift toward the direction of larger diffraction angle. This is mainly because the N atom enters into the nano SiC crystal and substitutes carbon to form N-doped nanocrystal. The covalent radius of N (0.075 nm) is less than that of C atom (0.077 nm), which leads to the decrease of lattice constant and the shift of XRD peak toward the larger diffraction angle. Apparently, a peak at $2\theta = 26.6^\circ$ is detected in both PDC-SiCN and PDC-SiC, which is corresponding to the diffraction peak of the in situ formed graphite due to the residual carbon existing in the PDC products [18,19].

The empirical formula of PDC-SiCN ceramics which is calculated according to the element composition is shown in Table 1. With the increase of annealing temperature from 900 °C to 1400 °C, the C/Si atom ratio decreases from 1.18 to 1, which indicates the carbon content is slightly decreased. The C/Si ratio exceeds 1 when PDC-SiCN ceramics is annealed below 1200 °C, which implies the existence of free carbon. According to XRD result, free carbon still exists in the form of graphite in PDC-SiCN ceramics when annealed at 1400 °C, although the C/Si ratio is 1. There is still 28 mol% N in PDC-SiCN ceramics when annealed at 1400 °C. Besides the amorphous SiCN, the N atoms may also exist in SiC nano-crystal, leading to the formation of N-doped SiC nano-crystal. According to XRD and element analysis, the PDC-SiCN ceramics annealed at 900 °C and 1200 °C are composed of graphite and amorphous SiCN, while that annealed at 1400 °C is composed of N-doped SiC nano-crystal, graphite and amorphous SiCN. PDC-SiC ceramics annealed at 1400 °C are composed of SiC nano-crystal, graphite, and amorphous SiC.

3.2. Microstructure and electrical conductivity of Si_3N_4–SiCN composite ceramics

Fig. 3 shows the morphologies of porous Si_3N_4 ceramic and samples S1, S2 and S3. Apparently, the rod-like grains of

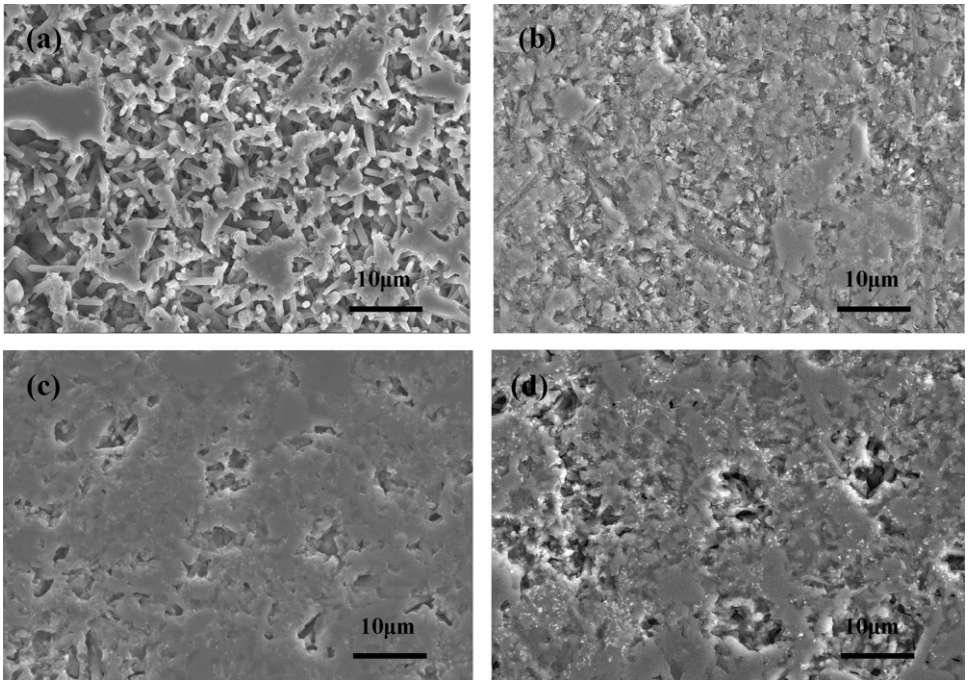

Fig. 3. SEM micrograph of (a) porous Si_3N_4 ceramic, (b) sample S1, (c) sample S2, and (d) sample S3.

porous Si_3N_4 ceramics intercross with each other to form through-pores. After PIP, the pores are occupied by SiCN ceramic, which results in the decrease of the porosity and the increase of the density of samples. As shown in Table 1, the open porosity decreases from 46% to 20% and the density increases from 1.7 g/cm^3 to 2.5 g/cm^3 after PIP at 900 °C. After annealed at 1200 °C and 1400 °C, the open porosity and density of samples are nearly the same.

The electrical conductivities of samples S1, S2 and S3 are shown in Table 1. Si_3N_4 is an electrically insulating material, the conductivity of which is below 10^{-13} S/cm [20]. After PIP and heat-treatments, the conductivities of samples S1, S2, and S3 are increased to 7.6×10^{-12}, 4.9×10^{-10} and 1.2×10^{-8} S/cm, respectively. For samples S1 and S2, the increases of conductivity are mainly ascribed to the formation of graphite in PDC-SiCN ceramics. When annealed at 1400 °C, the N-doped SiC nano-crystal appears in PDC-SiCN ceramics. Therefore, the increase of conductivity of sample S3 is due to the formation of N-doped SiC nano-crystal in PDC-SiCN ceramics.

3.3. Dielectric properties of Si_3N_4–SiCN composite ceramics

Complex permittivity ($\varepsilon = \varepsilon' - j\varepsilon''$) is an important parameter to characterize the dielectric properties of materials. The real part of permittivity (ε') is related to polarization, and the imaginary part (ε'') represents the dielectric loss of a material [8]. Although high ε'' implies good microwave absorbing properties, too high permittivity is harmful to the impendence match and results in strong reflection and weak absorption [21]. Fig. 4 shows the real and imaginary permittivity of porous Si_3N_4, samples S1, S2, and S3 at X-band. For each sample, the real permittivity and imaginary permittivity do not change apparently over the whole frequency range. The real and imaginary permittivity of porous Si_3N_4 with a porosity of 46% is 3.7 and 4.68×10^{-3}. After PIP, the largest real permittivity of samples is up to 8.9, which is 2.4 times higher than that of porous Si_3N_4. The average imaginary permittivity of samples S1 and S2 is 0.2 and 0.3, respectively. However, the average imaginary permittivity of sample S3 is up to 1.8, which is 6 times more than those of samples S1 and S2, and 385 times more than that of porous Si_3N_4. As shown in Fig. 5, the permittivity of PDC-SiC/paraffin sample with a PDC-SiC content of 20 vol.% was detected for comparison. The average real and imaginary permittivities of sample are 6.1 and 0.75 respectively, which are smaller than those of sample S3. According to the XRD analysis, elemental analysis and conductivity analysis, the increase in dielectric loss of sample S3 is mainly ascribed to the formation of N-doped SiC nano-crystal in PDC-SiCN ceramics.

An important mechanism of dielectric loss is Debye relaxation, which can be characterized by ε'–ε'' relationship, displaying as Cole–Cole semicircle with each semicircle corresponding to a Debye relaxation [22]. According to Debye theory, the Cole–Cole semicircle can be plotted according to the following equation:

$$(\varepsilon' - \varepsilon_\infty)^2 + (\varepsilon'')^2 = (\varepsilon_s - \varepsilon_\infty)^2 \quad (2)$$

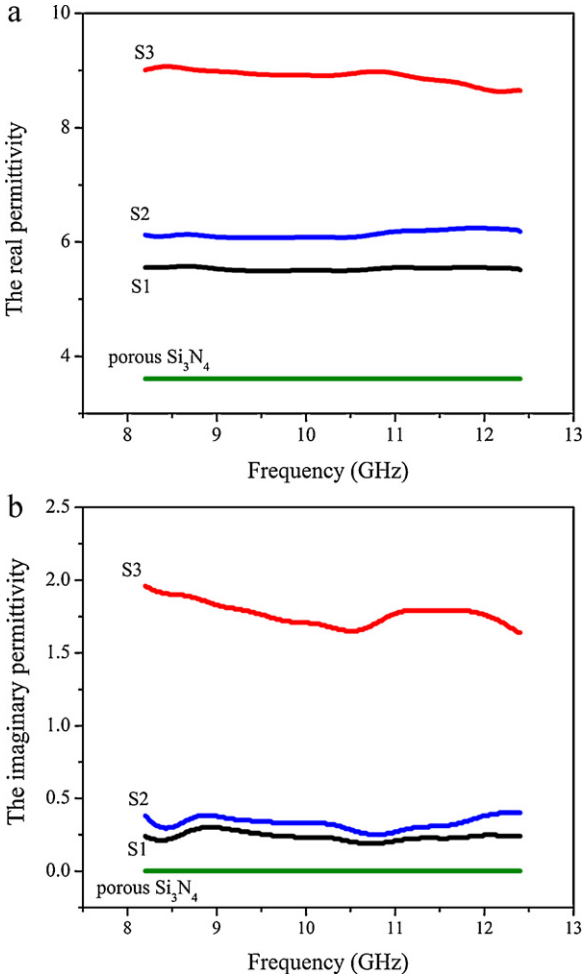

Fig. 4. The permittivity of porous Si_3N_4 ceramic, and samples S1, S2, S3, (a) real permittivity, (b) imaginary permittivity.

where ε_s is static permittivity, and ε_∞ is the relative dielectric permittivity at high frequency limit. The Cole–Cole semicircle of porous Si_3N_4 is a dot in the plot, which shows no Debye relaxation, so its imaginary permittivity is as low as 4.68×10^{-3}. As shown in Fig. 6, there are inconspicuous

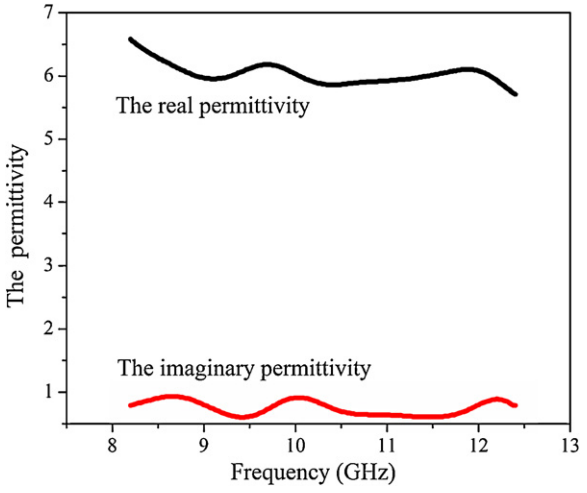

Fig. 5. The permittivity of SiC/paraffin sample.

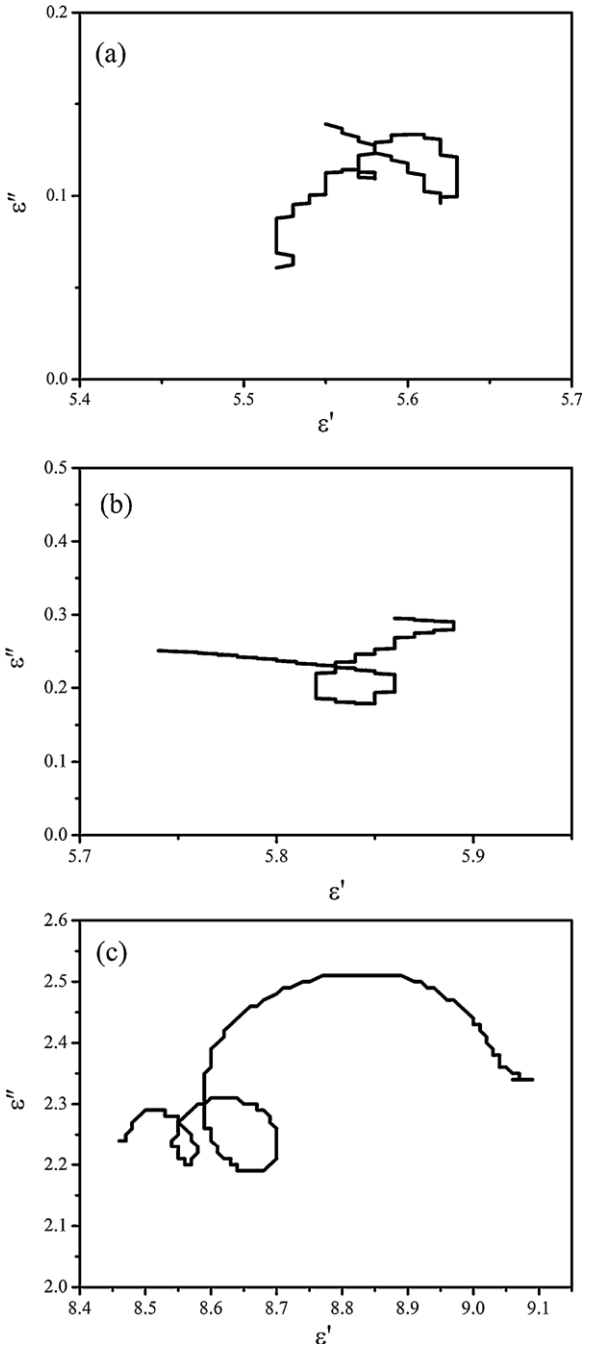

Fig. 6. Cole–Cole semicircles of (a) sample S1, (b) sample S2, and (c) sample S3.

but existing Cole–Cole semicircles for samples S1 and S2, which means weak Debye relaxation. Obviously, sample S3 shows three typical Cole–Cole semicircles, which indicate a ternary dielectric Debye relaxation behavior, so its imaginary permittivity is up to 1.8. The ternary dielectric Debye relaxation could lead to a promising perspective for microwave absorption materials [22].

In the present work, there is a great deal of Si and C vacancies in SiCN ceramics due to the doping of nitrogen [8]. These vacancies together with positive charge can form electric dipoles, which generate polarization relaxation and dissipate the energy under alternating electromagnetic field. Besides, there are a large number of nano-grain boundaries in the PDC-SiCN ceramics, which can dissipate the microwave energy for space charge polarization and relaxation [23]. Moreover, the graphite is formed through the reaction between Si–CH=CH_2 and Si–CH=CH_2 in the precursor. Therefore, it is supposed there exists a great deal of defects in the graphite, which results in the dielectric polarization relaxation. The similar phenomenon has been found in a reduced graphite oxide [22]. Briefly, the ternary semicircles of sample S3 are ascribed to the electric dipoles relaxation and grain boundaries relaxation of N-doping SiC nano-crystal, and the dielectric relaxation of defects in graphite. The weak Debye relaxation of samples S1 and S2 is due to the dielectric polarization relaxation of the in situ formed graphite.

4. Conclusions

Porous Si_3N_4–SiCN composite ceramics are successfully fabricated through PIP method using polysilazane as precursor and porous Si_3N_4 as preform at 900 °C. The phase composition of SiCN can be altered by changing the annealing temperature, by which the dielectric properties of Si_3N_4–SiCN composite ceramics are changed. The N-doped SiC nano-crystals begin to appear in SiCN at 1400 °C, and the SiC grain size is about 1.5 nm. The in situ-formed graphite exists in SiCN ceramic when annealed below 1400 °C. After PIP, the average real and imaginary permittivity of porous Si_3N_4 ceramics is increased from 3.7 and 4.68×10^{-3} to 8.9 and 1.8, respectively. The improvement of dielectric loss of samples is due to the appearance of N-doped SiC nano-crystal after annealed at high temperatures.

Acknowledgments

This work was supported by the fund of the state key laboratory of solidification processing in Northwestern Polytechnical University (No. KB200920) and the 111 Project (B08040).

References

[1] D.D.L. Chung, Electromagnetic interference shielding effectiveness of carbon materials, Carbon 39 (2001) 279–285.
[2] X. Zhang, X. Dong, H. Huang, Y. Liu, W. Wang, X. Zhu, B. Lv, J. Lei, Microwave absorption properties of the carbon-coated nickel nanocapsules, Appl. Phys. Lett. 89 (2006) 053115.
[3] M. Han, H.P. Lu, L.J. Deng, Control of gigahertz permeability and permittivity dispersion by means of nanocrystallization in FeCo based nanocrystalline alloy, Appl. Phys. Lett. 97 (2010) 192507.
[4] D. Zhao, F. Luo, W. Zhou, Microwave absorbing property and complex permittivity of nano SiC particles doped with nitrogen, J. Alloys Compd. 490 (2010) 190–194.
[5] R. Wongmaneerung, P. Singjai, R. Yimnirun, S. Ananta, Effects of SiC nanofibers addition on microstructure and dielectric properties of lead titanate ceramics, J. Alloys Compd. 475 (2009) 456–462.
[6] H. Zhang, J. Zhang, H. Zhang, Electromagnetic properties of silicon carbide foams and their composites with silicon dioxide as matrix in X band, Compos. A: Appl. Sci. 38 (2007) 602–608.

[7] X. Yu, W. Zhou, F. Luo, W. Zheng, D. Zhu, Effect of fabrication atmosphere on dielectric properties of SiC/SiC composites, J. Alloys Compd. 479 (2009) L1–L3.
[8] X. Li, L. Zhang, X. Yin, Z. Yu, Mechanical and dielectric properties of porous Si_3N_4–SiC(BN) ceramic, J. Alloys Compd. 490 (2010) L40–L43.
[9] B. Zhang, J. Li, J. Sun, S. Zhang, H. Zhai, Z. Du, Nanometer silicon carbide powder synthesis and its dielectric behavior in the GHz range, J. Eur. Ceram. Soc. 22 (2002) 93–99.
[10] D. Zhao, H. Zhao, W. Zhou, Dielectric properties of nano Si/C/N composite powder and nano SiC powder at high frequencies, Physica E 9 (2001) 679–685.
[11] H. Jin, M. Cao, W. Zhou, S. Agathopoulos, Microwave synthesis of Al-doped SiC powders and study of their dielectric properties, Mater. Res. Bull. 45 (2010) 247–250.
[12] C. Haluschka, C. Engel, R. Riedel, Silicon carbonitride ceramics derived from polysilazanes, part II. Investigation of electrical properties, J. Eur. Ceram. Soc. 20 (2000) 1365–1374.
[13] R. Raj, L. An, S. Shah, Oxidation kinetics of an amorphous silicon carbonitride ceramic, J. Am. Ceram. Soc. 84 (2001) 1803–1810.
[14] S.R. Shah, R. Raj, Nanoscale densification creep in polymer-derived silicon carbonitrides at 1350 °C, J. Am. Ceram. Soc. 84 (2001) 2208–2212.
[15] X. Li, L. Zhang, X. Yin, L. Feng, Q. Li, Effect of chemical vapor infiltration of SiC on the mechanical and electromagnetic properties of Si_3N_4–SiC ceramic, Scr. Mater. 63 (2010) 657–660.
[16] X. Yin, X. Li, L. Zhang, L. Cheng, Y. Liu, T. Pan, Microstructure and mechanical properties of Lu_2O_3-doped porous silicon nitride ceramics using phenolic resin as pore-forming agent, Int. J. Appl. Ceram. Technol. 7 (2010) 391–399.
[17] H. Li, L. Zhang, L. Cheng, Y. Wang, Z. Yu, M. Huang, H. Tu, H. Xia, Effect of polycarbosilane structure on its final ceramic yield, J. Eur. Ceram. Soc. 28 (2008) 887–891.
[18] L. Ya, E. Kroke, R. Riedel, C. Fasel, C. Gervais, F. Babonneau, Thermal cross-linking and pyrolytic conversion of poly(ureamethylvinyl)silazanes to silicon-based ceramics, Appl. Organomet. Chem. 15 (2001) 820–832.
[19] S. Zhu, S. Ding, H. Xi, R. Wang, Low-temperature fabrication of porous SiC ceramics by preceramic polymer reaction bonding, Mater. Lett. 59 (2005) 595–597.
[20] Z. Guo, G. Blugan, T. Graule, M. Reece, J. Kuebler, The effect of different sintering additives on the electrical and oxidation properties of Si_3N_4–$MoSi_2$ composites, J. Eur. Ceram. Soc. 27 (2007) 2153–2161.
[21] R. Che, L. Peng, X. Duan, Q. Chen, X. Liang, Microwave absorption enhancement and complex permittivity and permeability of Fe encapsulated within carbon nanotubes, Adv. Mater. 16 (2004) 401–405.
[22] C. Wang, X. Han, P. Xu, X. Zhang, Y. Du, S. Hu, J. Wang, X. Wang, The electromagnetic property of chemically reduced grapheme oxide and its application as microwave absorbing material, Appl. Phys. Lett. 98 (2011) 072906.
[23] X. Yin, Y. Xue, L. Zhang, L. Cheng, Dielectric, electromagnetic absorption and interference shielding properties of porous yttria-stabilized zirconia/silicon carbide composites, Ceram. Int. 38 (2012) 2421–2427.